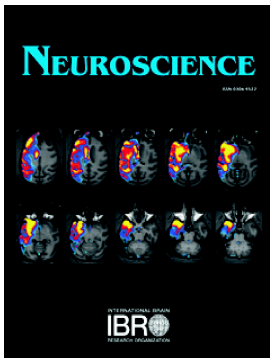


# Modulation of acid sensing ion channel dependent protonergic neurotransmission at the mouse calyx of Held

Carlota González-Inchauspe, María Natalia Gobetto, Osvaldo D. Uchitel

PII: S0306-4522(19)30263-5
DOI: https://doi.org/10.1016/j.neuroscience.2019.04.023
Reference: NSC 19011

To appear in: *Neuroscience*

Received date: 18 December 2018
Revised date: 4 April 2019
Accepted date: 5 April 2019

Please cite this article as: C. González-Inchauspe, M.N. Gobetto and O.D. Uchitel, Modulation of acid sensing ion channel dependent protonergic neurotransmission at the mouse calyx of Held, Neuroscience, https://doi.org/10.1016/j.neuroscience.2019.04.023

# Modulation of acid sensing ion channel dependent protonergic neurotransmission at the mouse calyx of Held.

Carlota González-Inchauspe, María Natalia Gobetto & Osvaldo D. Uchitel

*Instituto de Fisiología, Biología molecular y Neurociencias (IFIBYNE) CONICET. Departamento de Fisiología, Biología Molecular y Celular "Dr. Héctor Maldonado", Facultad de Ciencias Exactas y Naturales, Universidad de Buenos Aires. Ciudad Universitaria. (C1428EGA) Ciudad Autónoma de Buenos Aires, Argentina.*

Correspondence should be addressed to Dr. Carlota González-Inchauspe

E-mail: carlota@fbmc.fcen.uba.ar

Instituto de Fisiología, Biología molecular y Neurociencias (IFIBYNE) UBA-CONICET

Facultad de Ciencias Exactas y Naturales. Edificio IFIBYNE Ciudad Universitaria. (C1428EGA) Ciudad Autónoma de Buenos Aires, Argentina.

Phone: (+54-11) 4576 3368

FAX: (+54-11) 4576 3321

**Keywords**

Acid sensing ion channel (ASIC); Protons; Histamine, Spermine; Lactate; Glutamatergic synaptic transmission; Synaptic plasticity; Calyx of Held

## Abstract

Acid-sensing ion channels (ASICs) regulate synaptic activities and play important roles in neurodegenerative diseases. It has been reported that homomeric ASIC-1a channels are expressed in neurons of the medial nucleus of the trapezoid body (MNTB) of the auditory system in the CNS. During synaptic transmission, acidification of the synaptic cleft presumably due to the co-release of neurotransmitter and $H^+$ from synaptic vesicles activates postsynaptic ASIC-1a channels in mice up to 3 weeks old. This generates synaptic currents (ASIC1a-SCs) that add to the glutamatergic excitatory postsynaptic currents (EPSCs). Here we report that neuromodulators like histamine and natural products like lactate and spermine potentiate ASIC1a-SCs in an additive form such that excitatory ASIC synaptic currents as well as the associated calcium influx become significantly large and physiologically relevant. We show that ASIC1a-SCs enhanced by endogenous neuromodulators are capable of supporting synaptic transmission in the absence of glutamatergic EPSCs. Furthermore, at high frequency stimulation (HFS), ASIC1a-SCs contribute to diminish short term depression (STD) and their contribution is even more relevant at early stages of development. Since ASIC channels are present in almost all type of neurons and synaptic vesicles content is acid, the participation of protons in synaptic transmission and its potentiation by endogenous substances could be a general phenomenon across the central nervous system.

## Introduction

In the brain, neural activity gives rise to extracellular and intracellular pH shifts that originate from several mechanisms (Chesler 2003). The synaptic cleft is subject to changes in proton concentration due to transmembrane fluxes and to spontaneous or action potential evoked fusion of synaptic vesicles. Vesicular pH is low (Miesenböck et al. 1998) as a result of $H^+$-ATPase activity which generates an electrochemical gradient that drives transport of neurotransmitter into the vesicle (Liu and Edwards 1997). During exocytosis, protons are released together with neurotransmitters into the synaptic cleft. Synaptic activity is associated with a transient decrease in extracellular pH in hippocampal slices (Krishtal 2003) and vesicular acidification is lost and regained after endocytosis (Miesenböck et al. 1998), consistent with release of protons into the synaptic cleft. In photoreceptors terminals, DeVries (2001) has estimated that the release of vesicular protons during exocytosis causes an acidification of the synaptic cleft from 7.5 to 6.9. Cho and von Gersdorff (2014) and Vincent et al. (2018) reported evidence for proton release from bullfrog auditory hair ribbon synapses. They estimated a fast release of between 600-1300 $H^+$ per synaptic ribbon via multivesicular exocytosis which inhibits presynaptic $Ca^{2+}$ channels, reducing the next wave of transmitter release. This modulation takes place in synapses from mature animals where a compact active-zone topography with $Ca^{2+}$channel rows flanked by two rows of docked vesicles is present. Much less is known about pH changes during synaptic transmission at non-ribbon synapses. At central synapses, like the calyx of Held, $Ca^{2+}$ current inhibition by proton release has not been detected (Vincent et al. 2018). At such synapses, with hundreds of disperse active zones, exocytosis is evoked by a rapid activation of $Ca^{2+}$ currents in response to invading action potentials; and normally involves the release of only one or a few vesicles at each active zone (Meyer et al. 2001). It has also been demonstrated that the number of docked vesicles per active zone (AZ) and the release probability decrease with age. These changes led to AZs that are less prone to multivesicular release (Taschenberger et al 2002). Nevertheless, although magnitudes of synaptic cleft acidification during transmission are small, they seem to be sufficient to activate acid sensing ion channels (ASICs, Du et al. 2014, Kreple et al. 2014, González-Inchauspe et al. 2017).

ASICs are $H^+$-gated cation channels, which belong to the epithelial sodium channel/degenerin superfamily (Krishtal 2003, Waldmann and Lazdunski 1998). Molecular cloning has identified several distinct ASIC subunits (Hanukoglu and Hanukoglu 2016). Of those, ASIC1a, ASIC2a and ASIC2b show widespread expression throughout the central and peripheral nervous systems, whereas ASIC1b and ASIC3 are largely restricted to the peripheral nervous system (Wemmie et al 2006, Kellenberger and Schild 2015). ASICs are implicated in a variety of pathological conditions such as neurotoxicity following ischemia, anxiety and pain (Wemmie et al 2006, Kellenberger and Schild 2015, Xiong et al. 2004, Baron and Lingueglia 2015, Deval and Lingueglia 2015). The subunit ASIC-1a forms heteromeric channels with ASIC-2a, and also $Ca^{2+}$-permeable homomeric channels (Xiong et al. 2004, Yermolaieva et al. 2004, Lingueglia et al. 1997, Wu et al. 2004). ASIC-1a is enriched in synaptosomal fractions, which are expressed in dendritic spines, where channels interact with postsynaptic scaffolding proteins like PSD-95 and PICK1 (protein interacting with C kinase 1) and also with NMDA receptors and voltage-gated $Ca^{2+}$ channels (Hruska-Hageman et al. 2002, Wemmie et al.

2002, Zha 2013). ASIC-1a channels display pronounced desensitization. As a consequence, slow acidification makes ASICs insensitive to further changes of pH (Gründer and Pusch 2015). Thus, significant ASIC-mediated current are generated only in response to a fast decrease in pH, like fast acidifications occurring during synaptic transmission.

We have recently shown (González-Inchauspe et al. 2017) that ASIC-1a mediated synaptic currents (ASIC1a-SCs) are activated during synaptic transmission at the synapse formed by the calyx of Held and the Medial Nucleus of the Trapezoid Body (MNTB).The inhibition of ASIC1a-SCs by psalmotoxin-1 and the absence of these currents in knock-out mice for ASIC-1a subunit (ASIC1a $^{-/-}$) suggest that homomeric ASIC-1as are mediating these currents in MNTB neurons. A significant characteristic of these homomeric ASIC-1a channels is their permeability to $Ca^{2+}$ (Gründer and Pusch 2015). As a consequence, the activation of postsynaptic ASIC-1a during high-frequency stimulation of the presynaptic nerve terminal leads to a Psalmotoxin-1-sensitive increase in intracellular $Ca^{2+}$ in MNTB neurons, which is independent of glutamate receptors and is absent in neurons from ASIC1a $^{-/-}$ mice (González-Inchauspe et al. 2017).

The ASIC1a-SC contribution to the total EPSC amplitude is very small (less than 1%), a fact that rises doubts about their role as depolarizing currents capable of altering postsynaptic excitability. Therefore, we were interested to search for endogenous substance that could potentiate ASIC1a-SCs. Diverse natural products have been shown to potentiate ASIC currents tested on heterologous systems (Baron and Lingueglia 2015, Nagaeva et al. 2016). However, their effect on native systems has not been tested. Here we report that neuromodulators like histamine and natural products like lactate and spermine potentiate nerve evoked ASIC1a-SCs in an additive form such that excitatory ASIC1a-SCs as well as the associated calcium influx become significantly large and physiologically relevant. Furthermore, we found that the contribution of ASIC1a-SCs to the total synaptic current is larger during high frequency stimulation (HFS) steady state depression suggesting a relevant role of these currents in synaptic communication when glutamate signalling is diminished.

## Experimental Procedures

### *Animal model and preparation of brainstem slices*.

Either sex mice C57BL/6 of P9 to P23 days were killed by decapitation and their brain was removed. The brainstem was mounted in the Peltier chamber of an Integraslice 7550PSDS vibrating microslicer (Campden Instruments Limited, UK). Transverse slices of 300 μm thicknesses were cut in an ice-cold low-sodium artificial cerebrospinal fluid (aCSF) where NaCl was replaced by 250 mM of sucrose and $MgCl_2$ and $CaCl_2$ concentrations were 2.9 mM and 0.1 mM respectively. They were then transferred to an incubation chamber containing normal bicarbonate aCSF with low calcium (0.1 mM $CaCl_2$ and 2.9 mM $MgCl_2$) at 37 ºC for half an hour. This study was carried out in strict accordance with the recommendations in the Guide for the Care and Use of Laboratory Animals of the National Institutes of Health. The protocol was approved by the Committee on the Ethics of Animal Experiments of the University of Buenos Aires (Protocol Nº: 112-2018).

### *Electrophysiology recordings*

Slices were transferred to a recording chamber with aCSF containing (mM): NaCl 125, KCl 2.5, $NaHCO_3$ 26, $NaH_2PO_4$ 1.25, glucose 10, ascorbic acid 0.5, myo-inositol 3, sodium pyruvate 2, $MgCl_2$ 1 and $CaCl_2$ 2. The pH was 7.3 when gassed with 95% $O_2$-5% $CO_2$. Neurons were visualized using Nomarski optics on a BX50WI (Olympus, Japan) microscope, with a 60X/0.90 NA water immersion objective lens (LUMPlane FI, Olympus). In those experiments that required an aCSF with high buffering capacity that prevented pH changes, a 10 mM Hepes-based aCSF solution was used, containing (in mM): NaCl 128, KCl 2.5, $CaCl_2$ 2, $MgCl_2$ 1, glucose 15, sucrose 15, Hepes 10, ascorbic acid 0.5, myo-inositol 3 and sodium pyruvate 2. The pH was brought to 7.3 with NaOH and it was gassed with $O_2$.When lactate 15 mM was added to the bath solution $CaCl_2$ and $MgCl_2$, were adjusted to 2.35 mM and 1.12 mM respectively.

Patch pipettes were pulled from borosilicate glass (Harvard Apparatus, GC150F-15, UK). Electrodes had resistances of 2.9 to 3.2 MΩ when filled with internal solution of the following composition (mM): CsCl 110, Hepes 40, TEA-Cl 10, $Na_2$phosphocreatine 12, EGTA 0.5, MgATP 2, LiGTP 0.5 and $MgCl_2$ 1. PH was adjusted to 7.3 with CsOH. To block $Na^+$ currents and avoid postsynaptic action potentials, 10 mM *N*-(2,6-diethylphenylcarbamoylmethyl)-triethyl-ammonium chloride (QX-314) was added to the pipette solution. Patch clamp recordings were obtained using Multiclamp 700B amplifier (Axon CNS, Molecular Devices), Digidata 1440A (Axon CNS, Molecular Devices) and pClamp 10.6 software.

$H^+$-gated, ASIC-1a mediated synaptic currents (ASIC1a-SCs) and glutamatergic excitatory postsynaptic currents (EPSCs) on MNTB neurons were measured by whole cell voltage-clamping. Postsynaptic action potentials (APs) were recorded in loose patch configuration, where no gigaseal is formed and no break-in into the cell is performed. Data were sampled at 100 kHz and filtered at 6 kHz (Low pass Bessel). Whole-cell membrane capacitances (13-20 pF) and series (access) resistances (5-12 MΩ) were registered from the amplifier after compensation of the transient generated by a 10 ms voltage step, and compensated by 50-60%.

EPSCs, ASIC1a-SCs and postsynaptic APs were evoked by stimulating the globular bushy cell axons in the trapezoid body using a bipolar platinum electrode placed in the midline and applying square pulses (0.1 ms, 1-5 mA) through an isolated constant-current stimulator (Model DS3, Digitimer Ltd., UK). To isolate ASIC1a-SCs, AMPA, NMDA, $GABA_A$ and glycine receptors were blocked by the corresponding inhibitors: 2,3-dioxo-6-nitro-7-sulfamoylbenzo(f)quinoxaline (NBQX, 20 μM), (2R)-amino-5-phosphonovaleric acid (D-APV, 50 μM), bicuculline (20 μM) and strychnine (2 μM). During exogenous application of histamine, lactate and/or spermine, ASIC1a-SCs were measured at a frequency of 0.1 Hz, and a minimum of 20 ASIC1a-SC recordings in each condition were considered to calculate the average.

***Fluorescence measurements***

For $Ca^{2+}$ image acquisition we used a BX51WI upright microscope with a 60X objective lens (Olympus) and an EMCCD camera (AndoriXon, Oxford Instruments), together with cell-M System Coordinator/ cell-R Real Time controller software. MNTB neurons were loaded with the high affinity $Ca^{2+}$ indicator Fluo 8 in salt form, added to a final concentration of 100 μM to the CsCl-based patch solution with no EGTA. Neurons were voltage-clamped at -70 mV and ASIC1a-SCs were recorded during presynaptic terminals at 150 Hz while simultaneously measuring the fluorescence emitted by the Fluo 8. The excitation

and emission wavelengths were 488 nm and 515 nm, respectively. Off-line image processing was performed using ImageJ. To analyze time-dependent fluorescence changes we normalized mean fluorescence values as follows. First, the average $Ca^{2+}$ fluorescence signal in MNTB cells was 'background-corrected' by subtraction of the average measured signal from an extracellular region. Mean background-corrected fluorescence measured in the first images before presynaptic stimulation (Fo, line base before activating ASIC-1a channels) was subtracted to the background-corrected fluorescence measured in each image frame during the protocol and finally normalized to Fo. This procedure subtracts auto-fluorescence and present data as ΔF/Fo.

***Data Analysis and Statistics***

Data analysis was done using Clampfit 10.6 (Molecular Devices, USA), Sigma Plot 10.0, SigmaStat 3.5 and Excel 2007 (Microsoft). Average data are expressed and plotted as mean± sem. Statistical significance was determined using paired or unpaired Student's *t*-test or One Way Repeated Measures Analysis of Variance, ANOVA, plus Student-Newman-Keulspost-hoc test.

The concentration dependence of histamine action on ASIC1a-SCs evoked in MNTB neurons was fitted by the Hill equation: $I = I_M/[1 + (IC_{50}/C)^{nH}]$, where $I_M$ is the maximum current potentiation, C is the histamine concentration, $IC_{50}$ the concentration for half current potentiation, and $n_H$ is the Hill coefficient.

## Results

*Developmental changes in ASIC1a-SCs at the calyx of Held synapse*

We measured EPSCs in MNTB neurons clamped at -70 mV while electrically stimulating the presynaptic axons. After pharmacologically blocking AMPA, NMDA, GABA and glycine receptors with NBQX (20 μM), D-APV (50 μM), bicuculline (20 μM), and strychnine (2 μM), respectively, we could detect ASIC1a-SCs, which we previously reported sensitive to ASIC blocker amiloride and to the specific ASIC-1a inhibitor psalmotoxin-1. ASIC1a-SCs were also absent at the $ASIC1a^{-/-}$ mice and were greatly reduced by an extracellular aCSF with high buffering capacity (Hepes 10 mM) that prevented pH changes (González-Inchauspe et al 2017). We observed developmental changes in the activation of ASIC-1a channels during synaptic transmission. ASIC-SCs in young mice (P9-P10) have mean amplitudes of 36 ± 4 pA (n = 7) which were not significantly different from those in more mature mice in the range P13-P19 (41 ± 3 pA, n = 12, p = 0.1, Student´s *t*-test). In contrast, we did not observe ASIC1a-SCs during presynatic stimulation in seven of ten MNTB neurons from mice between P20 and P23. In three neurons we could detect ASIC1a-SCs with mean amplitudes of 12.8 ± 0.6 pA, which were inhibited by 10 nM of Psalmotoxin-1 (fig. 1a). Nevertheles, ASIC-1a channels were present in MNTB neurons of P20-P23 mice, since proton ($H^+$)-gated, ASIC1a-mediated currents (fig. 1b) were activated during local acidification by pressure applications of a 2 s duration puff of 5 mM Hepes/5 mM MES-based aCSF solution at pH = 6.0 using a micropipette (1.5-2 MΩ resistance) connected to a Picrospritzer (Intracel LTD, UK). These currents have peak amplitudes of 260 ± 26 pA (n = 10) and were inhibited to 80 ± 4 % by Psalmotoxin-1 (n = 3, p = 8 $10^{-4}$, Student´s *t*-test, control vs Psalmotoxin-1). So, adult mice of more than 21 postnatal days express functional homomeric ASIC-1a channels that can be activated by protons, but at these ages these channels seem not to participate in synaptic

transmission at the calyx of Held. This suggests that ASIC channels are removed from the synaptic area but remain in extra-synaptic locations. There is also evidence (Taschenberger et al 2002) that single active zones (AZs) at the calyx of Held may release more than one vesicle in young mice (higher release probability) and only one vesicle at the more mature mice (when the number of AZs is larger and the release probability is lower). This lack of multivesicular release may be another reason for the small ASIC1a-SC activation by afferent fiber stimulation in more mature calyx. All subsequent experiments were done in P13-P19 mice, except when specifically indicated.

*ASIC1a-SCs are affected by carbonic anhydrase enzymatic activity.*

To further prove that ASIC1a-SCs were activated by nerve evoked released protons, we tested the effects of altering pH-buffering by inhibiting the enzyme carbonic anhydrase (CA) (Chesler 2003). CA is one of the main regulators of tissue pH which catalyzes the rapid and reversible conversion of $CO_2$ and water to $HCO_3^-$ and $H^+$ (Shah et al. 2005). Inhibition of CA results in a reduced pH buffering capacity, therefore assuming that higher proton concentration last longer. As shown in fig. 2a, acetazolamide (AZT), an inhibitor of the CA, increased ASIC1a-SC amplitudes by 29 ± 3% ($p = 4.5\ 10^{-4}$, Student´s paired *t*-test, n = 4, P14-P17 mice). Mean and individual values of ASIC1a-SCs amplitudes from MNTB neurons in the absence and in the presence of AZT are presented in fig. 2b. These results strongly reinforced the concept that in physiological conditions the nerve evoked release of protons drops the pH of the cleft and activates postsynaptic ASIC-1a channels.

*Modulation of ASIC1a-SCs by histamine at the calyx of Held-MNTB synapse.*

Histamine is a neurotransmitter synthesized by neurons in the tuberomammillary nucleus of the posterior hypothalamus (Sherin et al. 1998). Histamine-containing nerve fibers project to many structures in the brain (Panula and Nuutinen 2013) and histaminergic circuits regulate numerous physiological functions and behaviours, including sleep-wake activities, circadian and feeding rhythms, learning, and memory (Parmentier et al 2002, Dere et al 2003, Haas and Panula 2003, Haas et al 2008).

It has recently been reported that synthetic hydrophobic monoamines potentiate or inhibit ASIC currents in subunit-specific manner (Nagaeva et al. 2016, Shteinikov et al. 2017). Histamine selectively potentiates responses of ASIC-1a channels and its action is particularly pronounced at minor acidifications, which cause small responses (Nagaeva et al. 2016).

At MNTB neurons, we observed that histamine (0.5 mM) added to the aCSF increased ASIC1a-SCs (after blocking AMPA, NMDA, GABA and Glycine receptors) as shown in fig 3a left. To confirm that these currents were due to endogenous acidification, we used Hepes 10 mM-based aCSF, obtaining a substantial reduction (75 ± 7 %, p = 0.017, Student´s paired *t*-test, n = 2) on the amplitudes of ASIC1a-SCs. Mean values of ASIC1a-SC amplitudes in the absence and in the presence of histamine plus paired data for each individual MNTB neuron are presented in fig 3a right. Mean potentiation of ASIC1a-SC amplitudes by histamine was 84 ± 4 % ($p = 1.5\ 10^{-6}$, Student´s paired *t*-test, n = 10).

Histamine increased ASIC1a-SC amplitudes in a dose-dependent manner. The concentration-response relationship for histamine is shown in fig 3b (n = 5). Fitting the Hill equation to the experimental data indicates a maximum enhancement of 145 ± 12 %, and an $IC_{50}$ of 0.48 ± 0.08 mM.

To corroborate that histamine was acting directly on ASIC-1a channels and not through histamine receptors, the same experiments were performed inhibiting histamine receptors H1 and H2 with mepiramine (10 μM) and tiotidine (10 μM). In these conditions, histamine increased ASIC1a-SC amplitudes by 86 ± 14 % (p = 0.012, Student´s paired *t*-test, n = 3), a value not significantly different from that obtained in the absence of H1 and H2 histamine receptor antagonists (fig 3c).

*Histamine increased intracellular $Ca^{2+}$ influx through ASIC-1a channels in MNTB neurons.*

An attribute of homomeric ASIC-1a channels is their permeability to $Ca^{2+}$ (Xiong et al 2004, Yermolaieva et al. 2004). To estimate transient changes in [$Ca^{2+}$] produced by the opening of ASIC-1a channels, the high affinity $Ca^{2+}$ indicator Fluo 8 was loaded into MNTB neurons. Upon binding to calcium, this dye exhibits an increase in fluorescence emission intensity. We stimulated presynaptic terminals at 150 Hz during 0.4 s and recorded ASIC1a-SCs while simultaneously measuring the fluorescence emitted by the Fluo 8. Fluorescent images were taken every 50 ms (first 15 images before stimulation as line base) in normal bicarbonate-based aCSF containing AMPA, NMDA, GABA and glycine receptors. Only neurons with small leak currents (less than 50 pA) and so stable resting membrane potential were considered in the analysis. Fig 3d left shows an example of ASIC1a-SCs evoked by 150 Hz presynaptic stimulation in the absence and in the presence of histamine in the aCSF. The bar graph displays mean and individual values amplitudes of the first ASIC1a-SC in the train, before and after histamine bath application. Mean enhancement by histamine was 79 ± 11% (p = 1.1 $10^{-3}$, Student´s paired *t*-test, n = 5). Figure 3d right shows the average ratio of dye fluorescence intensity ΔF/Fo as a function of time, showing a $Ca^{2+}$ dependent increase in fluorescence due to ASIC-1a channel activation during the stimulation train. Before histamine application, the maximum ΔF/Fo was 3.4 ± 0.2 % (squares, control). Histamine (1 mM) enhanced the change in fluorescence to a peak value ΔF/Fo of 5.9 ± 0.3 % (triangles, n = 5). The inset shows mean and individual peak $Ca^{2+}$ dependent fluorescence ratios ΔF/Fo before and after histamine bath application, indicating an augmentation of 77 ± 14% by histamine (p = 9.4 $10^{-4}$, Student´s paired *t*-test, n = 5).

*Lactate and spermine also potentiates ASIC-1a mediated currents*

During rest the interstitial concentration of lactate is determined by glycolytic production in astrocytes and mitochondrial consumption in neurons, both of which are controlled by neuronal activity (Barros 2013). During intensive exercise the metabolism becomes anaerobic and lactate is released into the blood and enters into the brain tissue (van Hall 2010). Blood lactate concentrations following exercise can rise to ~20 mM; however, common levels range between 10 and 15 mM in healthy active subjects (Philp et al. 2005). In pathological conditions, for example during brain ischemia, the switch to anaerobic respiration leads to production of lactate, which can rise from a resting value of 1-2 mM to concentrations of 12-20 mM in the extracellular space (Schurr & Rigor 1997). Immke & McCleskey (2001) have shown that 15 mM of lactate

potentiated currents through neuronal ASICs via a mechanism that chelates $Ca^{2+}$ and increases the sensitivity to protons (Immke & McCleskey 2001). The effect of lactate on ASIC1a-SCs evoked by presynaptic stimulation in MNTB neurons was investigated. Sample recordings of ASIC1a-SCs are presented in fig 4a left before and after adding 15 mM of lactate to the aCSF. $Ca^{2+}$ and $Mg^{2+}$ concentrations in the aCSF were modified to 2.35 mM and 1.12 mM to maintain the same free $Ca^{2+}$ and $Mg^{2+}$ concentration when 15 mM lactate was present (Immke & McCleskey 2001). Mean and individual values of ASIC1a-SC amplitudes in the absence and in the presence of lactate are depicted in fig 4a right. Lactate enhanced ASIC1a-SC amplitudes by 56 ± 7 % ($p = 1.7\ 10^{-4}$, Student´s paired *t*-test, n = 6). Simultaneous application of histamine and lactate increased ASIC1a-SC amplitudes by 140 ± 20 % (fig 4b, $p = 3\ 10^{-3}$, Student´s paired *t*-test, n = 3).

The polyvalent cation spermine modulates different ion channels and its extracellular concentration can significantly vary (Pegg 2014). Natural polyamines like spermine are synthesized and released upon brain trauma (Fage et al. 1992, Paschen et al. 1992). Spermine exerts a potentiating effect on the activity of ASIC-1b and ASIC-1a channels (Babini et al 2002). Spermine reduces the desensitization of ASIC-1a in the open state, but also accelerates the recovery after desensitization in response to repeated acid stimuli (Babini et al 2002). The concentration of spermine in secretory granules and nerve terminals from ox neurohypophyses has been calculated to be 0.26 and 0.52 mM, respectively (Kroigaard et al 1992). We observed that spermine (0.25 mM) increases ASIC1a-SCs by 53 ± 5 % ($p = 6.5\ 10^{-5}$, Student´s paired *t*-test, n = 8). Fig 4c shows representative recordings and amplitude values of ASIC1a-SCs in MNTB cells before and after application of spermine.

Remarkable, spermine does not block the potentiating effect of the other endogenous ligands mentioned above. Addition of lactate (15 mM) and histamine (1 mM) on spermine treated neurons increase ASIC1a-SCs up to 221 ± 18 % of the original value at room temperature ($p = 4\ 10^{-4}$, Student´s paired *t*-test, n = 4). Recordings of ASIC1a-SCs after sequentially applying each modulator are depicted in fig 4d left. A high concentration of intracellular $Ca^{2+}$ buffer (HEPES 10 mM-based aCSF) greatly reduces the proton activated ASIC current. Amplitude values of ASIC1a-SCs in the absence of any modulator and in the presence of spermine, spermine plus lactate and spermine + lactate + histamine are shown in fig 4d right (n = 4 NMTB neurons).

*Contribution of ASIC1a-SCs currents to EPSCs during HFS*

High frequency stimulation (HFS) at the calyx of Held-MNTB synapse caused short term depression (STD): EPSC amplitudes decreased during the train of stimuli until they reached a steady state. We investigated the contribution of postsynaptic ASIC-1a channels during HFS (100 Hz, 20 stimuli) by comparing EPSC amplitudes at the depressed steady state condition, measured sequentially in control conditions, under the effect of histamine and during the incubation with a high buffer capacity aCSF (Hepes 10 mM). Since there are developmental changes in synaptic plasticity, with young mice undergoing stronger STD than adult ones due to glutamate receptors desensitization (Koike-Tani et al. 2008), it is reasonable to suppose that ASIC contribution will be more relevant in developing mice. Therefore, studies were done in young and more mature mice for comparison. Recordings of EPSCs during HFS for P9-P10 mice are

presented in fig 5a. Plots of mean EPSC amplitudes as a function of time during 100 Hz stimulation, fitted by a single exponential decay function, are shown in fig 5b left (n = 6). Individual values of EPSC amplitudes at the steady state measured sequentially in each condition at 6 MNTB neurons are presented in fig 5b right (top), together with the mean values (all normalized to the amplitude of the first EPSC in the train). There is a reduction of 9.5 ± 0.7 % in EPSC amplitudes at the steady state during HFS when ASIC-1a channel activation is blocked by strong pH buffering with HEPES 10 mM ($p = 3\ 10^{-6}$, Student´s paired *t*-test, n = 6). On the other hand, histamine enhanced EPSC amplitudes at the end of the stimuli by 10.3 ± 0.8 % with respect to control conditions ($p = 4\ 10^{-5}$, Student´s paired *t*-test, n = 6) and by 22 ± 2 % compared to inhibition of acidification by Hepes 10 mM-based aCSF ($p = 8\ 10^{-6}$, Student´s paired *t*-test, n = 6).

To a lesser extent, pair pulse ratio (PPR) of EPSCs is also affected by ASIC-SCs. Individual and mean values of PPR in control conditions, under the effect of histamine and in Hepes 10 mM are shown in fig 5b right (bottom). There is a reduction of 4.6 ± 0.9 % in PPR when ASIC-1a channel activation is blocked by strong pH buffering with HEPES 10 mM ($p = 1.5\ 10^{-3}$, Student´s paired *t*-test, n = 6). Histamine enhanced PPR by 5.4 ± 1.3 % with respect to control conditions ($p = 2.3\ 10^{-3}$, Student´s paired *t*-test, n = 6) and by 10.6 ± 2.1 % compared to inhibition of acidification by Hepes 10 mM-based aCSF ($p = 1.3\ 10^{-3}$, Student´s paired *t*-test, n = 6).

In more mature mice (P13-P19), contribution of ASIC-1a to EPSCs in the course of STD is smaller, but still significant. Fig 5c left depicts the time course of EPSC amplitudes during 100 Hz synaptic activity fitted by single exponential decay functions. Normalized values of EPSC amplitudes at the steady state for 6 MNTB neurons in each condition are presented in fig 5c right (top), together with mean values. In Hepes 10 mM-based aCSF EPSC amplitudes at steady state during HFS were reduced by 3.9 ± 0.9 % compared to control conditions ($p = 2\ 10^{-3}$, student´s paired *t*-test, n = 7). Histamine enhanced EPSC amplitudes at the end of the stimuli by 3.7 ± 0.9 % with respect to control conditions ($p = 3.3\ 10^{-3}$, Student´s paired *t*-test, n = 7) and by 8 ± 2 % compared to inhibition of acidification by Hepes 10 mM-based aCSF ($p = 2.5\ 10^{-3}$, Student´s paired *t*-test, n = 7). Individual and mean values of PPR in control conditions, under the effect of histamine and in Hepes 10 mM are shown in fig 5c right (bottom). Inhibition of ASIC-1a channel activation by Hepes 10 mM reduced PPR by 2.5 ± 0.3 % ($p = 10^{-4}$, Student´s paired *t*-test, n = 7). Histamine enhanced PPR by 2.5 ± 0.2 % with respect to control conditions ($p = 2\ 10^{-5}$, Student´s paired *t*-test, n = 7) and by 5.2 ± 0.5 % compared to inhibition of acidification by Hepes 10 mM-based aCSF ($p = 2.5\ 10^{-5}$, Student´s paired *t*-test, n = 7).

Since STD is highly temperature dependent (Kushmerick et al. 2006), the same experiments were repeated in P13-P19 mice at a physiological temperature of 36ºC in normal aCSF with 1.2 mM $CaCl_2$ (Borst 2010) and at a stimulation frequency of 300 Hz (fig 6a,b). The inhibition of ASIC-1a channel activation using Hepes 10 mM-based aCSF reduced EPSC amplitudes at the HFS steady state by 4.0 ± 0.7 % compared to control conditions ($p = 6\ 10^{-5}$, Student´s paired *t*-test, n = 6). Histamine enhanced EPSC amplitudes at the end of the stimuli by 3.4 ± 0.4 % with respect to control conditions ($p = 2\ 10^{-4}$, Student´s paired *t*-test, n = 6) and by 7.6 ± 0.1 % compared to the effect of Hepes 10 mM-based aCSF ($p = 1.7\ 10^{-7}$, Student´s paired *t*-test, n = 6). Concerning PPR, inhibition of ASIC-1a channel activation by Hepes 10 mM reduced PPR by 2.2 ± 0.2 % ($p = 5.6\ 10^{-5}$, Student´s paired *t*-test, n = 6). Histamine enhanced PPR by 2.3 ± 0.5 % with respect to control

conditions ($p = 2\ 10^{-3}$, Student´s paired *t*-test, n = 6) and by 4.7 ± 0.6 % compared to inhibition of acidification by Hepes 10 mM-based aCSF ($p = 2\ 10^{-4}$, Student´s paired *t*-test, n = 6).

Therefore, the participation of ASIC1a-SCs in synaptic plasticity during HFS is present in different experimental conditions including those resembling physiological conditions (normal aCSF solution with 1.2 mM CaCl2 at 36ºC).

*Potentiated ASIC1a-SCs are capable to elicit action potentials.*

To investigate the relevance of ASIC1a-SCs on synaptic transmission in physiological conditions we studied the capability of ASIC1a-SCs to elicit action potentials (APs) in conditions where all other postsynaptic receptors were blocked. Slices were incubated at 36ºC in normal aCSF solution with 1.2 mM $CaCl_2$ (Borst 2010). To test the reliability of synaptic transmission we use "loose-patch" extracellular recordings: MNTB neurons were loosely patched by a micropipette filled with extracellular media, without obtaining a gigaseal and no break-in into the neuron was performed. Because the recording is extracellular, the internal environment of the postsynaptic cell is undisturbed and so no changes in the firing properties of the neuron are introduced. APs at the MNTB neurons were elicited by nerve stimulation at 0.2 Hz and 300 Hz. The large glutamatergic EPSCs bring postsynaptic neurons well above threshold for firing and thus allow high reliability in synaptic transmission, firing one action potential in response to each synaptic current as shown in fig 7a. When glutamate AMPA and NMDA receptors as well as GABA and glycine receptors were blocked, nerve stimulation failed to generate APs (Fig 7b). However, in the presence of 0.6 mM of histamine, two of eight cells fired a few AP when stimuli were delivered at 300 Hz. Furthermore, in 6 of 8 MNTB neurons incubated with histamine (0.5 mM) plus spermine (0.25 mM), several APs were generated as shown in fig 7c.

In order to elucidate the magnitudes of the ASIC1a-SCs that were able to trigger APs, we measured these currents in whole-cell voltage clamp using aCSF with the same concentration of $CaCl_2$ (1.2 mM) at the same temperature (36ºC), before and after adding histamine (0.5 mM) plus spermine (0.25 mM) in the bath solution. Fig 7d, left shows an example of ASIC1a-SCs in the conditions mentioned above, together with similar recordings at room temperature (25ºC) for comparison. The rise in temperature accelerates the kinetics and increases the amplitudes of ASIC1a-SCs. Mean half width and rise time decrease from 0.92 ± 0.08 ms and 0.26 ± 0.03 ms at 25°C to 0.43 ± 0.04 ms and 0.13 ± 0.01 ms at 35°C ($p = 1.8\ 10^{-5}$ and $p = 1.7\ 10^{-5}$, Student´s *t*-test, respectively, n = 12). The increase in amplitude due to temperature effect was 150 ± 10 % ($p = 8\ 10^{-5}$, Student´s *t*-test, n = 12). Mean charges of ASIC1a-SCs are display in fig 7d right, in the absence and in the presence of histamine plus spermine at both temperatures. In summary, the effect of temperature and histamine plus spermine enhanced ASIC1a-SC charge from 23 ± 4 pA.ms to 93 ± 13 pA.ms, representing an increase of 308 ± 41 % ($p = 8\ 10^{-7}$, Student´s *t*-test, n = 6) that allow ASIC1a-SCs to elicit APs. These experiments prove the concept that in the absence of glutamatergic currents, potentiated ASIC1a-SCs are sufficient to depolarize the postsynaptic neuron over the AP threshold in physiological conditions.

**Discussion**

In recent years it has been demonstrated that ASIC-1a are postsynaptic receptors to protons released during synaptic transmission. In amygdala (Du et al. 2014), nucleus accumbens (Kreple et al. 2014) and the calyx of Held (González-Inchauspe et al 2017) protons co-released with glutamate activate postsynaptic ASIC channels and generate ASIC1a-SCs mainly carried by $Na^+$ and in less proportion by $Ca^{2+}$ ions. We further prove this concept showing the ability of acetazolamide to increase the ASIC-dependent postsynaptic currents, strongly suggesting the role of pH in its activation and the release of protons from synaptic vesicles, the most likely source of protons. The ASIC currents were greatly reduced but not completely blocked by Psalmotoxin-1, although we use 10 times the $IC_{50}$ of the toxin. Thus, it is possible that a small number of heteromeric forms of ASICs, non sensitive to Psalmotoxin-1 are still active at the postsynaptic membrane.

Although protonergic neurotransmission is already established, its role in synaptic and network communication is not fully understood, mainly due to the small size of the synaptic ASIC currents compared with the glutamatergic synaptic currents. Our results showed that endogenous substances and neuromodulators are capable of potentiating ASIC1a-SCs in physiological conditions. Furthermore, we demonstrate that during HFS those potentiated currents significantly increase the amplitude of the EPSCs and could eventually compensate for a diminished glutamatergic signal.

Nagaeva et al. (2016) have reported that histamine potentiates ASIC-1a but no other isoforms expressed in chinese hamster ovary (CHO) cells. In CHO transfected with rat ASIC-1a, low-pH applications (from 7.3 to 6.5) induced ASIC1a-mediated currents that were potentiated by 120 ± 35% by histamine 1mM. Histamine action depended on the activating pH value. Increase of proton concentration reduced both affinity and efficacy of histamine. Histamine 1 mM caused 280 ± 40% potentiation at pH = 6.8, but at pH = 5.0 the effect was non-significant, suggesting that histamine causes a shift of the channel activation and so has no significant effect on the maximal response to acidification. We have confirmed the potentiating effect of histamine at the calyx of Held on native postsynaptic ASIC-1a receptors. To our knowledge, specific histaminergic innervation of the MNTB neurons has not been reported. Nevertheless, in other systems it has been considered that a high enough concentrations of histamine could be reached in the synaptic cleft as histamine concentration in synaptic vesicles can be as high as 670 mM (Borycz et al. 2015). The concentration used in our experiments was chosen in base of the concentration-response relationship for histamine observed for ASIC1a-SCs in MNTB neurons (fig 3b). Nagaeva et. al. (2016) show concentration dependencies of histamine action at different pH values, which reaches the saturation at concentrations greater than 1 mM. Our results indicate that histamine enhanced ASIC1a-SCs physiologically activated during synaptic transmission by 84 ± 4 %. Its action was independent of H1 or H2 histamine receptor blockers, suggesting that histamine is acting directly on the ASIC-1a channels, presumably by a direct binding to a proton binding site as postulated by Nagaeva et al. (2016). Our previous work revealed that ASIC1a-SCs are underlying the glutamatergic EPSCs at the calyx of Held (González-Inchauspe et al. 2017), although representing less than 1 % of the total current when the calyx is stimulated at low frequency. Histamine exerts a potentiating effect which is perceptible when glutamatergic EPSCs are inhibited.

Recent studies have shown that certain endogenous ligands associated with ischemia, such us spermine and lactate (Immke and McCleskey 2001, Allen and Attwell 2002) can enhance ASIC-1a currents. Spermine, one of the endogenous polyamines synthesized by mammals from the diamine putrescine, interacts with acidic residues of different nature. Therefore, multiple actions have been suggested for these polycations, including modulation of the activity of ionic channels (Guerra et al 2016). Duan et al. (2011) have demonstrated that spermine exacerbates ischemic neuronal injury through sensitization of ASIC-1a channels. This unique modulation was explained by a reduced rate of desensitization of ASIC-1a channels from the open state and a shift of the steady state desensitization to lower pH. Babini et al. (2002) showed that 0.25 mM of spermine shifted the steady-state inactivation curve of ASIC1a and ASIC1b expressed in sensory neurons of the dorsal root ganglion, which would increase the number of available channels. Increasing the number of available channels would be especially relevant during tissue acidosis and may contribute to increased excitotoxicity during seizures and ischemia when the extracellular pH falls. Spermine (0.25 mM) enhanced proton (pH6.0)-induced currents in cultured cortical neurons from WT mice by 20% and in CHO cells transfected with homomeric ASIC1a or heteromeric 1a/2a channels by ~ 75% and ~ 40%, respectively. Instead, it has no effect in proton (pH6.0)-evoked currents mediated by homomeric ASIC1b, 2a, and 3 channels, or by heteromeric ASIC1a/1b and 1a/2b channels (Duan et al 2011). Thus, spermine specifically affects the two major forms of ASICs (1a, 1a/2a) known to be present in CNS neurons (Baron et al. 2002; Askwith et al. 2004). In cultured hippocampal neurons, a region known to be vulnerable to brain ischemia (Gao et al., 2005), the extent of potentiation of proton (pH6.0)-evoked currents was ~ 60% in rat and ~ 20% in mouse neurons (Duan et al 2011). This may be attributed to the difference in ASIC subunit composition (i.e., ratio of 1a to 1a/2a) in CNS neurons between the two species (Baron et al. 2008) and in different brain regions, an idea supported by the observation that spermine had larger enhancement effect on homomeric ASIC1a than heteromeric 1a/2a channels. Here, we have observed that spermine 0.25 mM increases ASIC1a-SCs evoked by nerve stimulation at the calyx of Held synapse by 53 ± 5 %.

Intense activity and hypoxia are factors that cause an increase in lactate production and concentration in the brain (Vannucci and Hagberg 2004). The role of extracellular lactate in enhancing the activity of ASICs through chelation of extracellular calcium is known to involve modulation of ASIC-1a (Immke and McCleskey 2001). Calcium ions block ASIC-1a channels as a result of competition between $Ca^{2+}$ and $H^{+}$ at the activation site (Immke and McCleskey 2003, Paukert et al. 2004) while lactate binds and diminishes extracellular free $Ca^{2+}$, thereby allowing the channel to open at lower $H^{+}$ concentrations (Immke and McCleskey 2003). Lactate (30 mM) facilitated exogenous pH 6-evoked ASIC-mediated currents by approximately 66% in carotid body glomus cells by chelating extracellular $Ca^{2+}$, and so, potentially sensitizing cardiac sensory neurons to sense ischemia (Tan et al. 2007, Poirot et al. 2006). Thus, the unique capacity of ASIC channels to integrate both $H^{+}$ and lactate suggests that they might be particularly important pH sensors during metabolic acidosis associated with tissue ischemia or maximal exercise. In dissociated dorsal root ganglion (DRG) sensory neurons from rats, ASIC currents evoked by a change in extracellular pH from 7.4 to 7.0 increased by 62% in the presence of 15 mM of lactate (Immke and McCleskey 2001). The response improved with lactate concentration and showed no saturation up to 30 mM. Modulation by lactate decreased

at more acidic pH and was lost at pH = 6.0. In cerebellar Purkinje cells, which express ASIC subunits 1a and 2a, 15 mM of lactate potentiated ASIC-mediated currents activated by a pH 6.7 solution by 25 ± 2% (Allen and Attwell 2002). In the present study, lactate 15 mM potentiated endogenous ASIC1a-SCs activated during synaptic transmission at the calyx of Held by 56 ± 7 % (n = 6).

Interestingly, we have observed that the potentiating effect of histamine, spermine and lactate are additive, suggesting that a combination of these factors could generate ASIC1a-SCs that could influence synaptic output and network communication. Indeed, we have demonstrate that in physiological conditions potentiation of ASIC1a-SCs can overcome a complete blockage of glutamatergic current since their activation is capable of triggering postsynaptic APs, therefore restoring functional synaptic communication based solely on protonergic neurotransmission. In our previous report (González Inchauspe et al. 2017), non potentiated ASIC1a-SCs were capable of eliciting postsynaptic action potentials. This apparent discrepancy could be explained because in the former experiments synaptic transmission was studied at room temperature, in conditions of higher external $Ca^{2+}$ concentration in the aCSF and dialyzed patch clamped postsynaptic cells with their resting potential set at -65mV. In the present work we attempted to investigate the effect of the protonergic transmission in a more physiological context. Therefore, we used loose patch recordings to do not interfere with the internal environment of the postsynaptic cell. Furthermore we use 1.2 mM of $Ca^{2+}$ in the external solution and experiments were done at 36º C. Nevertheless, the potentiated currents were measured in the presence of glutamate receptor blockers, an obvious non physiological setting which may increase the input resistant and favor a stronger depolarization of the postsynaptic neuron.

We have restricted our study to a few endogenous substances. Further work needs to be done to document that other endogenous substance like nitric oxide (Wang et al. 2012), arachidonic acid (Smith et al. 2007) or corticosterone (Xiong et al. 2013), known to facilitate ASIC currents in heterologous systems, are capable to potentiate the ASIC1a-SCs in a native system.

The participation of ASIC1a-SCs in the glutamatergic synaptic currents elicited by HFS at the calyx of Held was studied without glutamate receptor blockers in the bath. During HFS synaptic currents decrease in amplitude as a result of vesicle depletion and glutamate receptor desensitization (Koike-Tani et al. 2008, Regehr 2012), a phenomenon known as short term depression. The potentiating effect of histamine during the steady state depression was 3.7 ± 0.9 % in older animals and 9.5 ± 0.7 % in younger ones. Furthermore, by bathing the preparation with a high capacity pH buffer it is possible to evaluate the participation of histamine enhanced ASIC1a-SCs during the steady state depression, accounting to 8 ± 2 % in older mice and 22 ± 2 % in young animals. The large participation of ASIC1a-SCs in the total current during short term depression and its potentiation by histamine and possibly by other endogenous substances emphasize the relevance of protonergic transmission and suggest its possible participation during events like high frequency communication where glutamate receptors may desensitize while ASICs do not as shown by MacLean and Jayaraman (2016).

Our finding of histamine, spermine and lactate action on ASIC-1a and the participation of ASIC currents during high frequency synaptic transmission can be of considerable physiological importance. The role of histamine as a neurotransmitter is well known in both peripheral and central nervous systems. In the

brain, histaminergic neurons are located in the hypothalamic tuberomammillary nucleus from where they send projections to many brain areas (Panula and Nuutinen 2013). Thus, local and transient rising of histamine concentrations in specific brain areas can modulate ASICs and increase their currents to physiologically significant levels.

Since ASIC channels are present in almost all type of neurons and excitatory and inhibitory synaptic vesicles content is acidic, the participation of protons in synaptic transmission and its potentiation by endogenous substances could be a general phenomenon across the central nervous system.

**Acknowledgments**

This work was supported by PICT 2016-3642 from Agencia Nacional de Promoción Científica y Tecnológica (ANPCYT) and UBACYT 01/Q666 (20020130100666BA) from University of Buenos Aires granted to Dr O.D. Uchitel.

**Author´s contribution**

Osvaldo D. Uchitel: Conceptualization, Investigation, Funding acquisition, Proyect administration, Supervision, Validation, Writing: Review & Editing

Carlota González-Inchauspe: Conceptualization, Investigation, Formal Analysis, Writing: Original Draft Preparation, Review & Editing

Natalia Gobetto: Investigation, Validation, Formal Analysis, Writing: Review & Editing

**References**

Allen NJ and Attwell D. (2002) Modulation of ASIC channels in rat cerebellar Purkinje neurons by ischaemia-related signals. J. Physiol. 543 (Pt 2): 521-9.

Askwith CC, Wemmie JA, Price MP, Rokhlina T, Welsh MJ (2004) Acid sensing ion channel 2 (ASIC2) modulates ASIC1 $H^+$-activated currents in hippocampal neurons. J Biol Chem 279: 18296 -18305.

Babini E, Paukert M, Geisler HS and Grunder S. (2002) Alternative splicing and interaction with di-and polyvalent cations control the dynamic range of acid-sensing ion channel 1 (ASIC1). J. Biol Chem. 277 (44): 41597-41603.

Baron A, Waldmann R, Lazdunski M (2002) ASIC-like, proton-activated currents in rat hippocampal neurons. J. Physiol 539: 485- 494.

Baron A, Voilley N, Lazdunski M, Lingueglia E (2008) Acid sensing ion channels in dorsal spinal cord neurons. J. Neurosci 28: 1498 -1508.

Baron A and Lingueglia E. (2015) Pharmacology of acid-sensing ion channels -Physiological and therapeutical perspectives. Neuropharmacology 94: 19-35.

Barros LF. (2013) Metabolic signaling by lactate in the brain. Trends Neurosci. 36 (7): 396-404.

Borst JG. (2010) The low synaptic release probability in vivo. Trends Neurosci. 33 (6): 259-266.

Borycz JA, Borycz J, Kubo A, Kostyleva Rand Meinertzhagen IA (2003) Histamine Compartments of the Drosophila Brain With an Estimate of the Quantum Content at the Photoreceptor Synapse. J. Neurophysiol. 93: 1611-1619.

Chesler M. (2003) Regulation and modulation of pH in the brain. Physiol Rev. 83: 1183-221.

Cho S and von Gersdorff H. (2014) Proton-mediated block of Ca2+ channels during multivesicular release regulates short-term plasticity at an auditory hair cell synapse. J Neurosci. 34(48):15877-87.

Dere E, De Souza-Silva MA, Topic B, Spieler RE, Haas HL, Huston JP. (2003) Histidine-decarboxylase knockout mice show deficient nonreinforced episodic object memory, improved negatively reinforced water-maze performance, and increased neo- and ventro-striatal dopamine turnover. Learn Mem. 10 (6): 510-519.

Deval E, Lingueglia E. (2015) Acid-Sensing Ion Channels and nociception in the peripheral and central nervous systems. Neuropharmacology 94: 49-57.

DeVries SH. (2001) Exocytosed protons feedback to suppress the $Ca^{2+}$ current in mammalian cone photoreceptors. Neuron 32: 1107-1117.

Du J, Reznikov LR, Price MP, Zha XM, Lu Y, Moninger TO, Wemmie JA, Welsh MJ. (2014) Protons are a neurotransmitter that regulates synaptic plasticity in the lateral amygdala. Proc. Natl. Acad. Sci. USA. 111: 8961-8966.

Duan B, Wang YZ, Yang T, Chu XP, Yu Y, Huang Y, Cao H, Hansen J, Simon RP, Zhu MX, Xiong ZG, Xu TL. (2011) Extracellular spermine exacerbates ischemic neuronal injury through sensitization of ASIC1a channels to extracellular acidosis. J. Neurosci. 31 (6): 2101-2112.

Fage D, Voltz C, Scatton B and Carter C. (1992) Selective release of spermine and spermidine from the rat striatum by N-Methyl-d-Aspartate receptor activation in vivo. J. Neurochem. 58: 2170-2175.

Gao J, Duan B, Wang DG, Deng XH, Zhang GY, Xu L, Xu TL (2005) Coupling between NMDA receptor and acid-sensing ion channel contributes to ischemic neuronal death. Neuron 48: 635- 646.

González-Inchauspe C, Urbano FJ, Di Guilmi MN and Uchitel OD. (2017) Acid-Sensing Ion Channels Activated by Evoked Released Protons Modulate Synaptic Transmission at the Mouse Calyx of Held Synapse. J. Neurosci. 37 (10): 2589-2599.

Gründer S and Pusch M. (2015) Biophysical properties of acid-sensing ion channels (ASICs). Neuropharmacology 94: 9-18.

Guerra GP, Rubin MA, Mello CF. (2016) Modulation of learning and memory by natural polyamines. Pharmacol. Res. 112: 99-118.

Haas H and Panula P. (2003) The role of histamine and the tuberomamillary nucleus in the nervous system. Nat. Rev. Neurosci. 4 (2): 121-130.

Haas HL, Sergeeva OA, Selbach O. (2008) Histamine in the nervous system. Physiol. Rev. 88 (3): 1183-1241.

Hanukoglu I, Hanukoglu A. (2016) Epithelial sodium channel (ENaC) family: Phylogeny, structure-function, tissue distribution, and associated inherited diseases. Gene. 579 (2): 95-132.

Hruska-Hageman AM, Wemmie JA, Price MP, Welsh MJ. (2002) Interaction of the synaptic protein PICK1 (protein interacting with C kinase 1) with the non-voltage gated sodium channels BNC1 (brain $Na^+$ channel 1) and ASIC (acid-sensing ion channel). Biochem. J. 361 (Pt 3): 443-450.

Immke DC and McCleskey EW. (2001) Lactate enhances the acid-sensing $Na^+$ channel on ischemia-sensing neurons. Nat. Neurosci. 4 (9): 869-870.

Immke DC and McCleskey EW. (2003) Protons open acid-sensing ion channels by catalyzing relief of $Ca^{2+}$ blockade. Neuron 37 (1): 75-84.

Kellenberger S and Schild L. (2015) International Union of Basic and Clinical Pharmacology. XCI. structure, function, and pharmacology of acid-sensing ion channels and the epithelial $Na^+$ channel. Pharmacol Rev. 67 (1): 1-35.

Koike-Tani M, Kanda T, Saitoh N, Yamashita T, Takahashi T. (2008) Involvement of AMPA receptor desensitization in short-term synaptic depression at the calyx of Held in developing rats. J. Physiol. 586 (Pt 9): 2263-2275.

Kreple CJ, Lu Y, Taugher RJ, Schwager-Gutman AL, Du J, Stump M, Wang Y, Ghobbeh A, Fan R, Cosme CV, Sowers LP, Welsh MJ, Radley JJ, LaLumiere RT, Wemmie JA. (2014) Acid-sensing ion channels contribute to synaptic transmission and inhibit cocaine-evoked plasticity. Nat. Neurosci. 17: 1083-1091.

Krishtal O. (2003) The ASICs: signaling molecules? Modulators? Trends Neurosci. 26: 477-483.

Kroigaard M., Thams P. and Thorn NA. (1992) Polyamines in nerve terminals and secretory granules isolated from neurohypophyses. Acta Physiol. Scand. 146: 233-239.

Kushmerick C, Renden R and von Gersdorff H. (2006) Physiological Temperatures Reduce the Rate of Vesicle Pool Depletion and Short-Term Depression via an Acceleration of Vesicle Recruitment. The Journal of Neuroscience 26 (5): 1366 -1377

Lingueglia E, de Weille JR, Bassilana F, Heurteaux C, Sakai H, Waldmann R, Lazdunski M. (1997) A modulatory subunit of acid sensing ion channels in brain and dorsal root ganglion cells. J. Biol. Chem. 272 (47): 29778-83.

Liu Y, Edwards RH. (1997) The role of vesicular transport proteins in synaptic transmission and neural degeneration. Annu Rev Neurosci. 20: 125-156.

MacLean DM and Jayaraman V. (2016) Acid sensing ion channels are tuned to follow high frequency stimuli. J. Physiol. 594 (10): 2629-2645.

Meyer AC, Neher E, Schneggenburger R. (2001) Estimation of quantal size and number of f unctional active zones at the caly x of Held synapse by non-stationary EPSC variance analysis. J. Neurosci 21: 7889 -7900.

Miesenböck G, De Angelis DA, Rothman JE. (1998) Visualizing secretion and synaptic transmission with pH-sensitive green fluorescent proteins. Nature 394: 192-195.

Nagaeva E.I, Tikhonova TB, Magazanik LG, Tikhonov DB. (2016) Histamine selectively potentiates acid-sensing ion channel 1a. Neurosci. Lett. 632: 136-140.

Panula P and Nuutinen S. (2013) The histaminergic network in the brain: basic organization and role in disease. Nat .Rev. Neurosci. 14 (7): 472-87.

Parmentier R, Ohtsu H, Djebbara-Hannas Z, Valatx JL, Watanabe T, Lin JS. (2002) Anatomical, physiological, and pharmacological characteristics of histidine decarboxylase knock-out mice: evidence for the role of brain histamine in behavioral and sleep-wake control. J. Neurosci. 22 (17): 7695-7711.

Paschen W, Widmann R and Weber C. (1992) Changes in regional polyamine profiles in rat brains after transient cerebral ischemia (single versus repetitive ischemia), evidence for release of polyamines from injured neurons. Neurosci. Lett. 135: 121-124

Paukert M, Babini E, Pusch M, Gründer S. (2004) Identification of the $Ca^{2+}$ blocking site of acid-sensing ion channel (ASIC) 1: implications for channel gating. J Gen Physiol. 124 (4): 383-94.

Pegg AE (2014). The function of spermine. IUBMB Life 66 (1): 8-18.

Philp A, Macdonald AL, Watt PW (2005) Lactate–a signal coordinating cell and systemic function. J Exp Biol. 208: 4561- 4575

Poirot O, Berta T, Decosterd I, Kellenberger S. (2006) Distinct ASIC currents are expressed in rat putative nociceptors and are modulated by nerve injury. J Physiol. 576: 215-234.

Regehr WG. (2012) Short-term presynaptic plasticity. Cold Spring Harb. Perspect Biol. 4 (7): a005702.

Sherin JE, Elmquist JK, Torrealba F, Saper CB. (1998) Innervation of histaminergic tuberomammillary

neurons by GABAergic and galaninergic neurons in the ventrolateralpreoptic nucleus of the rat. J. Neurosci. 18(12): 4705-21.

Schurr A. & Rigor B M (1997). Brain anaerobic lactate production: a suicide note or a survival kit? Developmental Neuroscience 20: 348-357.

Shah GN, Ulmasov B, Waheed A, Becker T, Makani S, Svichar N, Chesler M and Sly WS. (2005) Carbonic anhydrase IV and XIV knockout mice: Roles of the respective carbonic anhydrases in buffering the extracellular space in brain. PNAS 102 (46) 16771-16776.

Shteinikov VY, Korosteleva A S, Tikhonova TB, Potapieva N N & Tikhonov DB. (2017) Ligands of histamine receptors modulate acid-sensing ion channels. Biochem Biophys Res Commun. 490(4): 1314-1318.

Smith ES, Cadiou H, McNaughton PA. (2007) Arachidonic acid potentiates acid-sensing ion channels in rat sensory neurons by a direct action. Neuroscience 145 (2): 686-98.

Tan ZY, Lu Y, Whiteis CA, Benson CJ, Chapleau MW and Abboud FM (2007) Acid-sensing ion channels contribute to transduction of extracellular acidosis in rat carotid body glomus cells. Circulation Research 101(10): 1009-1019.

Taschenberger H, Lea RM, Rowland KC, Spirou GA and Henrique von Gersdorff H (2002) Optimizing synaptic architecture and efficiency for high-frequency transmission. Neuron 36: 1127-1143.

van Hall G. (2010) Lactate kinetics in human tissues at rest and during exercise. Acta Physiol (Oxf) 199(4): 499-508.

Vannucci SJ and Hagberg H. (2004) Hypoxia-ischemia in the immature brain. J. Exp. Biol. 207 (Pt 18): 3149-3154.

Vincent PFY, Cho S, Tertrais M, Bouleau Y, von Gersdorff H and Dulon D.(2018) Clustered Ca2+ Channels Are Blocked by Synaptic Vesicle Proton Release at Mammalian Auditory Ribbon Synapses. Cell Rep. 25(12): 3451-3464.e3.

Waldmann R and Lazdunski M. (1998) H(+)-gated cation channels: neuronal acid sensors in the NaC/DEG family of ion channels. Curr. Opin. Neurobiol. 8 (3): 418-24.

Wang JQ, Chu XP, Guo ML, Jin DZ, Xue B, Berry TJ, Fibuch EE, Mao LM. (2012) Modulation of ionotropic glutamate receptors and Acid-sensing ion channels by nitric oxide. Front Physiol. 3: 164.

Wemmie JA, Chen J, Askwith CC, Hruska-Hageman AM, Price MP, Nolan BC, Yoder PG, Lamani E, Hoshi T, Freeman JH Jr, Welsh MJ. (2002) The acid-activated ion channel ASIC contributes to synaptic plasticity, learning, and memory. Neuron 34 (3): 463-77.

Wemmie JA, Price MP, Welsh MJ. (2006) Acid-sensing ion channels: advances, questions and therapeutic opportunities. Trends Neurosci. 29 (10): 578-86.

Wu LJ, Duan B, Mei YD, Gao J, Chen JG, Zhuo M, Xu L, Wu M, Xu TL. (2004) Characterization of acid-sensing ion channels in dorsal horn neurons of rat spinal cord. J. Biol. Chem. 279 (42): 43716-43724.

Xiong Z, Liu Y, Hu L, Ma B, Ai Y, Xiong C. (2013) A rapid facilitation of acid-sensing ion channels current by corticosterone in cultured hippocampal neurons. Neurochem. Res. 38 (7): 1446-1453.

Xiong ZG, Zhu XM, Chu XP, Minami M, Hey J, Wei WL, MacDonald JF, Wemmie JA, Price MP, Welsh MJ, Simon RP. (2004) Neuroprotection in ischemia: blocking calcium-permeable acid-sensing ion channels. Cell 118 (6): 687-698.

Yermolaieva O, Leonard AS, Schnizler MK, Abboud FM, Welsh MJ. (2004) Extracellular acidosis increases neuronal cell calcium by activating acid-sensing ion channel 1a. Proc. Natl. Acad. Sci. USA 101 (17): 6752-6757.

Zha XM. (2013) Acid-sensing ion channels: trafficking and synaptic function. Mol. Brain. 6, 1. doi: 10.1186/1756-6606-6-1.

## Figure legends

Fig 1. *Developmental changes in ASIC1a-SCs at the calyx of Held synapse*

**A.** Recordings of ASIC1a-SCs by presynaptic stimulation of the calyx of Held before (black, control) and after (dark blue) applying Psalmotoxin-1 (10 nM) in the aCSF from an MNTB neuron of a P15 (left) and a P23 mouse (right). MNTB neurons were voltage clamped at a holding potential of -70 mV and AMPA, NMDA, GABA and glycine postsynaptic receptors were blocked with NBQX (20 μM), D-APV (50 μM), bicuculline (20 μM) and strychnine (2 μM). The averages of 20 ASIC1a-SC recordings in each condition and the corresponding standard deviation are shown as thick traces.

**B**. Representative traces of $H^+$-gated, ASIC-1a mediated currents from a P23 mouse MNTB neuron during transient acidification (2 s) of the extracellular media from pH 7.3 to pH 6.0 (black trace) and the inhibitory effect of Psalmotoxin-1 (dark blue). MNTB neurons were whole cell patch clamped at a holding potential of -70 mV.

Fig 2. *Acetazolamide (AZT) modulates proton activated ASIC-1a homomers and potentiates their responses (ASIC1a-SCs) in MNTB cells of P13-P19 mice.*

**A.** Recordings of ASIC1a-SCs by presynaptic stimulation of the calyx of Held before (black, control) and after (green) applying AZT (0.25 mM) in the aCSF. Psalmotoxin-1 inhibited the enhanced ASIC1a-SCs (dark blue). Each trace is the average of 20 ASIC1a-SCs.

**B.** Mean peak amplitudes of ASIC1a-SCs in control conditions (45 ± 3 pA) and in the presence of AZT (59 ± 4 pA). Paired data for each MNTB neuron are also shown. AZT potentiated ASIC1a-SCs by 29 ± 3 % ($p = 4.5\ 10^{-4}$, Student´s paired *t*-test, n = 4).

Fig. 3. *Histamine enhances ASIC1a-SCs and $Ca^{2+}$ influx in MNTB neuron from P13-P19 mice.*

**A**. **Left**: Traces of ASIC1a-SCs before (black) and after (pink) applying histamine 0.5 mM in the aCSF. An extracellular solution with high pH-buffering capacity (Hepes 10 mM) reduced ASIC1a-SCs by 75 ± 7 % (dark blue, n = 2). **Right**: Mean amplitudes of ASIC1a-SCs in control conditions (44 ± 4 pA) and after histamine (82 ± 7 pA, n = 10). Paired data for each MNTB neuron are also shown ($p = 1.5\ 10^{-6}$, Student´s paired *t*-test, n = 10).

**B.** Concentration dependence of histamine effect, presented as % of ASIC1a-SC amplitudes before histamine application. Curves are fitted by a Hill equation. Maximum increment in ASIC1a-SC amplitudes is 145 ± 12 % and the $IC_{50}$ value is 0.48 ± 0.08 mM (n = 5).

**C**. *Histamine effect is not through histamine receptors but through ASIC-1a channels themselves*

**Left**. Recordings of ASIC1a-SCs before and after applying histamine 0.5 mM in the aCSF previously incubated with H1 and H2 histamine receptor antagonists. **Right**: even when H1 and H2 histamine receptors were inhibited, histamine increases ASIC1a-SC amplitudes from 38± 4 pA to 71 ± 9 pA (p = 0.012, Student´s paired *t*-test, n = 3). The enhancement (86 ± 14 %) is not significantly different from that shown in fig 3a.

**D.** *Intracellular $Ca^{2+}$ influx through ASIC-1a channels in MNTB neurons during high frequency stimulation (HFS) is increased by histamine.*

**Left**: Recordings of ASIC1a-SCs evoked by 150 Hz (0.4 s) stimulation of presynaptic axons after blockage of postsynaptic receptors with NBQX, D-APV, bicuculline and strychnine n MNTB neurons, before (black trace, control) and after (pink trace) applying histamine in normal aCSF. Bottom: amplitudes of the first ASIC1a-SC in the 150 Hz train during the intracellular $Ca^{2+}$ measurements, before (41 ± 3 pA) and after histamine bath application (74 ± 6 pA, p = 1.1 $10^{-3}$, Student´s paired *t*-test, n = 5).

**Right**: time course of Fluo 8 fluorescence emission ratio ΔF/Fo measured simultaneously to the electrophysiology recordings mentioned above in MNTB neurons (the dark pink bar indicates time of 150 Hz stimulation). During HFS a maximum increase in intracellular $Ca^{2+}$ of 3.1 ± 0.4 % (n = 5) is observed (black squares, control). Histamine enhances the peak increase of $Ca^{2+}$- dependent fluorescence to 5.7 ± 0.3 % (pink triangles, histamine, $p < 0.05$, One Way RM ANOVA). **Inset**: mean and individual peak $Ca^{2+}$ dependent fluorescence ratios ΔF/Fo before (3.4 ± 0.2 %) and after histamine bath application (5.9 ± 0.3 %, p = 9.4 $10^{-4}$, Student´s paired *t*-test, n = 5).

Fig. 4. *ASIC1a-SCs were increased by the effect of lactate and spermine in P13-P19 mice.*

**A. Left**: Recordings of ASIC1a-SCs in the absence (black, control) and in the presence of 15 mM of lactate (dark green). **Right**: ASIC1a-SCs have mean amplitudes of 45 ± 4 pA in control conditions and 70 ± 5 pA after lactate, representing an increase of 56 ± 7 % (n = 6). Paired data for individual MNTB neurons is shown (p = 1.7 $10^{-4}$, Student´s paired *t*-test, n = 6).

**B.** The additive effect of lactate and histamine applied sequentially increases ASIC1a-SC amplitudes from 52 ± 3 pA to 124 ± 8 pA (140 ± 20 %, p = 3 $10^{-3}$, Student´s paired *t*-test, n = 3).

**C. Left**: Recordings of ASIC1a-SCs in MNTB neurons before (black, control) and after (light blue) application of spermine (0.25 mM). **Right**: mean ASIC1a-SC amplitudes in the absence (control) and in the presence of spermine (0.25 mM) were 37 ± 4 pA and 57 ± 5 pA (n = 8) respectively, representing an enhancement of 53 ± 5% (p = 6.5 $10^{-5}$, Student´s paired *t*-test, n = 8).

**D. Left**: recordings of ASIC1a-SCs showing the effect of sequentially applying spermine (0.25 mM), lactate (15 mM) and histamine (1 mM) and the inhibition induced by the incubation with a HEPES 10 mM-based aCSF. **Right**: mean amplitudes of ASIC1a-SCs in the absence of any modulator (control: 38 ± 5 pA) and in the presence of spermine (56 ± 8 pA, p = 6 $10^{-3}$, Student´s paired *t*-test, n = 4), spermine plus lactate (83 ± 12 pA, p = 3.4 $10^{-3}$, Student´s paired *t*-test, n = 4) and spermine + lactate + histamine (120 ± 11 pA, p = 4 $10^{-4}$, Student´s paired *t*-test, n = 4). On average ASIC current amplitudes were increased by 221 ± 18 % (p = 4 $10^{-4}$, Student´s paired *t*-test, n = 4).

Fig 5. *ASIC1a-SCs contribute to reduce short term depression (STD) of glutamatergic EPSCs during high frequency synaptic transmission in young (P9-P10) and more mature (P13-P19) mice.*

**A**. Recording of AP-evoked EPSCs in MNTB neurons from young mice (P9-P10) during 100 Hz stimulation in normal aCSF (black), after enhancing ASIC1a-SCs by histamine 1 mM (pink) and when acidification is

inhibited by a high buffering capacity solution (Hepes 10 mM, dark blue). Inset: magnification of the 5$^{th}$ to 8$^{th}$ EPSCs showing the difference in amplitudes when STD reaches its steady state.

**B**. **Lef**t: time course of EPSC peak amplitudes during presynaptic stimulation at 100 Hz in the absence of histamine (control, squares symbols), after histamine (triangles) and in Hepes 10 mM-based aCSF (circles, n = 6). Amplitudes were normalized to the first EPSC amplitude in the train and data were fitted to single exponential decay functions. The inset shows data for the last EPSCs in the train with higher magnification. **Right, top**: Mean EPSC amplitudes at the end of the stimuli reach a steady state value of 11.8 ± 0.6 % (control), 13.0 ± 0.6 % (histamine) and 10.6 ± 0.5 % (Hepes 10 mM) of the first EPSC amplitude in the train (n = 6). Paired data for each MNTB neuron in each condition is also shown. There are significant differences between control and Hepes 10 mM ($p = 3\ 10^{-6}$, Paired Student´s *t*-test), control and Histamine ($p = 4\ 10^{-5}$, Paired Student´s *t*-test) and Histamine and Hepes 10 mM ($p = 8\ 10^{-6}$, Student´s paired *t*-test, n = 6).

**Bottom:** Mean PPRs are 0.39 ± 0.01 (control), 0.41 ± 0.01 (histamine) and 0.37 ± 0.01 % (Hepes 10 mM, n = 6). There are significant differences between control and Hepes 10 mM ($p = 1.5\ 10^{-3}$, Paired Student´s *t*-test), control and Histamine ($p = 2.3\ 10^{-3}$, Paired Student´s *t*-test) and Histamine and Hepes 10 mM ($p = 1.3\ 10^{-3}$, Student´s paired *t*-test, n = 6).

**C**. Same as in b) but from more mature mice (P13-P19). STD is smaller than in young mice and steady state EPSC amplitudes at the end of the stimuli represent 24.0 ± 3.3 % (control), 24.9 ± 3.4 % (histamine) and 23.1 ± 3.2 % (Hepes 10 mM) of the first EPSC amplitude in the train (n = 7). There are significant differences between control and Hepes 10 mM ($p = 2\ 10^{-3}$, Paired Student´s *t*-test), control and Histamine ($p = 3.3\ 10^{-3}$, Paired Student´s *t*-test) and Histamine and Hepes 10 mM ($p = 2.5\ 10^{-3}$, Student´s paired *t*-test, n = 7). PPRs are 0.63 ± 0.05 (control), 0.65 ± 0.05 (histamine) and 0.62 ± 0.05 (Hepes 10 mM, n = 7). There are significant differences between control and Hepes 10 mM ($p = 10^{-4}$, Paired Student´s *t*-test), control and Histamine ($p = 2\ 10^{-5}$, Paired Student´s *t*-test) and Histamine and Hepes 10 mM ($p = 2.5\ 10^{-5}$, Student´s paired *t*-test, n = 7).

Fig. 6. *ASIC1a-SC contribution to STD of glutamatergic EPSCs during high frequency synaptic transmission in P13-P19 mice at a physiological temperature of 36ºC in normal aCSF with 1.2 mM of* $Ca^{2+}$

**A**. Representative recording of AP-evoked EPSCs in MNTB neurons from P13-P19 mice during 300 Hz stimulation at a physiological temperature of 36ºC in normal aCSF solution with 1.2 mM $CaCl_2$ (black), after enhancing ASIC1a-mediated currents by histamine 1 mM (pink) and when acidification is inhibited by a high pH buffer capacity solution (Hepes 10 mM, dark blue). Inset: magnification of the last EPSCs in the train, showing the difference in amplitudes when STD reaches its steady state, in the three mentioned conditions.

**B**. **Lef**t: time course of EPSC peak amplitudes recorded in MNTB neurons during presynaptic stimulation at 300 Hz in the absence of histamine (control, squares symbols), after histamine (triangles) and in Hepes 10 mM-based aCSF (circles, n = 6). Amplitudes were normalized to the first EPSC amplitude in the train and data were fitted to single exponential decay functions. The inset shows data for the last EPSCs in the train with higher magnification. **Right, top**: the EPSC amplitudes at the end of the stimuli reach a steady state value of 35.1 ± 3.7 % (control), 36.4 ± 3.6 % (histamine) and 33.8 ± 3.8 % (Hepes 10 mM) of the first EPSC amplitude in the train (n = 6). Data for each MNTB neuron in each condition is also shown. There are

significant differences between control and Hepes 10 mM ($p = 6\ 10^{-5}$, Paired Student´s *t*-test), control and Histamine ($p = 2\ 10^{-4}$, Paired Student´s *t*-test) and Histamine and Hepes 10 mM ($p = 1.7\ 10^{-7}$, Student´s paired *t*-test, n = 6). **Bottom:** Mean PPRs are 0.77 ± 0.03 (control), 0.78 ± 0.03 (histamine) and 0.75 ± 0.03 (Hepes 10 mM, n = 6). Individual paired values are also depicted. There are significant differences between control and Hepes 10 mM ($p = 5.6\ 10^{-5}$, Paired Student´s *t*-test), control and Histamine ($p = 2\ 10^{-3}$, Paired Student´s *t*-test) and Histamine and Hepes 10 mM ($p = 2\ 10^{-4}$, Student´s paired *t*-test, n = 6).

Fig 7. *Enhanced ASIC1a-SCs are capable to elicit action potentials in physiological conditions in P13-P19 mice*

MNTB extracellular recorded APs (indicated by *) evoked by presynaptic stimulation at low (0.2 Hz) and high (300 Hz) frequency, in a brain slice incubated in aCSF with 1.2 mM $Ca^{2+}$ at 36ºC. Stimulation artifacts were diminished for better intelligibility.

**A**. Superimposed recordings at 0.2 Hz frequency stimulation (left) and a single record at 300 Hz frequency stimulation (right) in control conditions. There are no failures in triggering postsynaptic APs

**B**. Absolute failure to elicit postsynaptic APs after blocking AMPA, NMDA, $GABA_A$ and glycine receptors.

**c**. Histamine (0.5 mM) and spermine (0.25 mM) added to the aCSF increase ASIC1a-SC amplitudes so that they reach the threshold needed to trigger some postsynaptic APs in the MNTB neurons.

**C**. **Left**: Whole-cell patch clamp recordings of ASIC1a-SCs in MNTB neuron perfused in aCSF with 1.2 mM $CaCl_2$ before and after the addition of histamine (0.5 mM) and spermine (0.25 mM), at room temperature (25ºC) and physiological temperature (36ºC). **Right**: Mean ASIC1a-SC charge before (control, 23 ± 4 pA.ms at 25ºC and 40 ± 6 pA.ms at 36 ºC, $p = 6.6\ 10^{-4}$, Student´s *t*-test, n = 6) and under the effect of histamine plus spermine (53 ± 6 pA.ms at 25ºC and 92 ± 12 pA.ms at 36 ºC, $p = 9\ 10^{-3}$, Student´s *t*-test, n = 6).

## Highlights

* Acid-sensing ion channels (ASICs) regulate synaptic activities and play important roles in neurodegenerative diseases.
* Protonergic neurotransmission activates homomeric acid sensing ion channels 1a (ASIC-1a) at the mouse calyx of Held synapse.
* ASIC-1a mediated synaptic currents are enhanced by histamine and other endogenous neuromodulators like lactate and spermine.
* Enhanced ASIC1a-SCs contribute to synaptic transmission and plasticity, for instance, diminishing short-term depression.

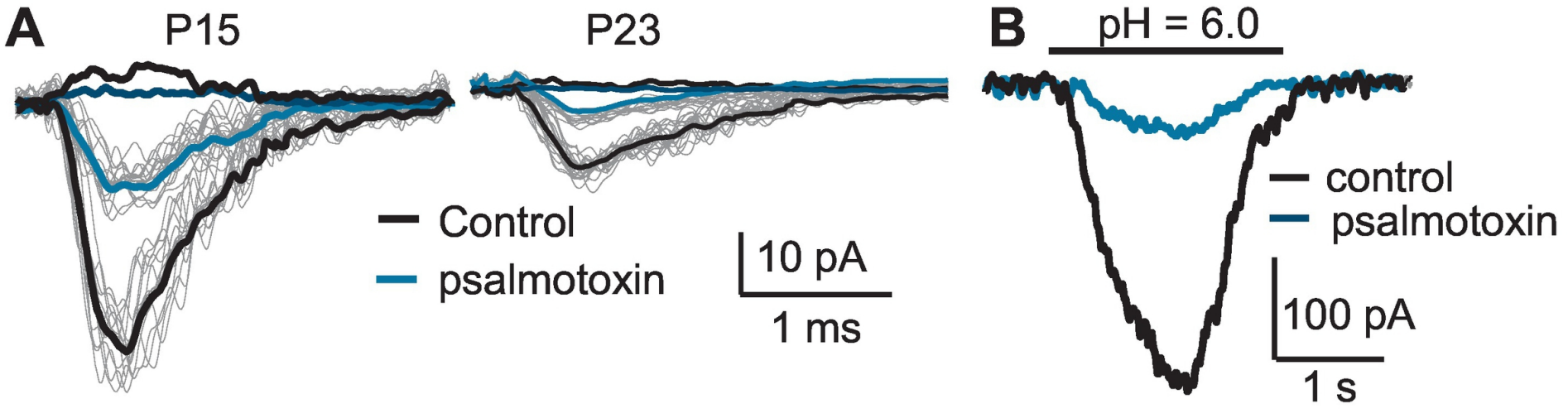
A
P15
P23
Control
psalmotoxin
10 pA
1 ms
B
pH = 6.0
control
psalmotoxin
100 pA
1 s

Figure 1

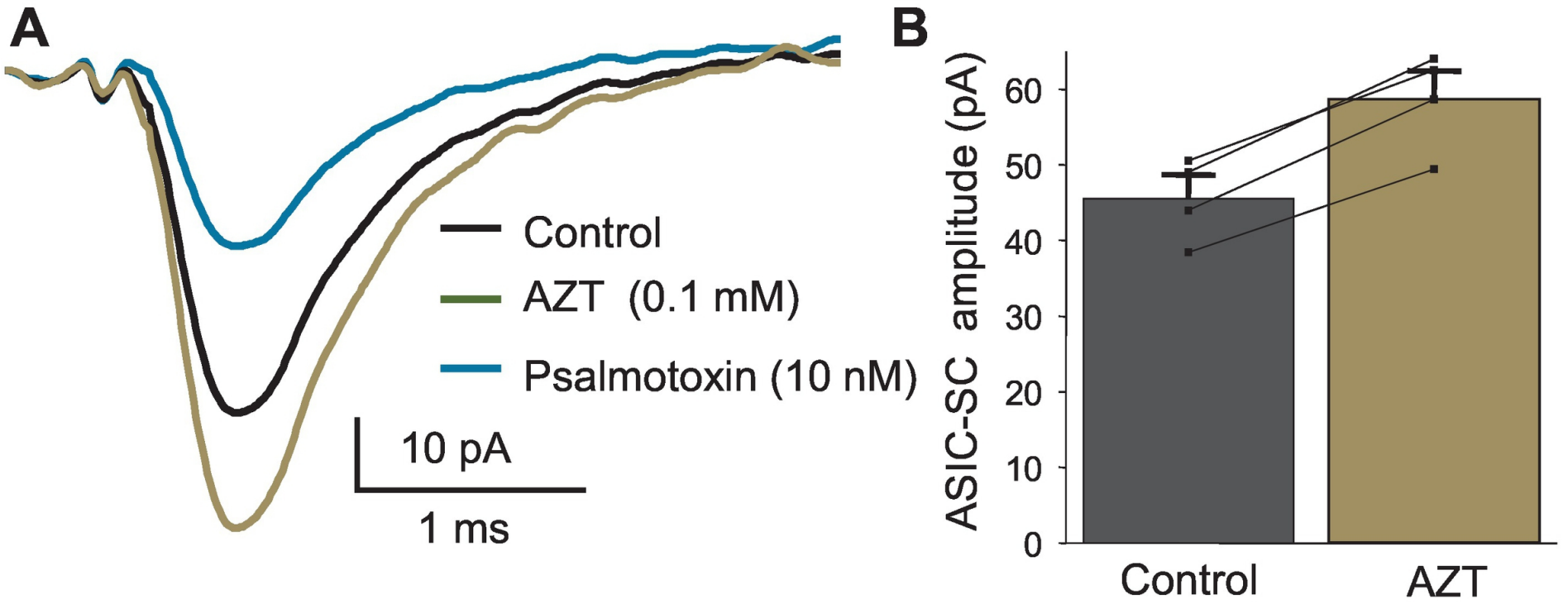
A
Control
AZT (0.1 mM)
Psalmotoxin (10 nM)
10 pA
1 ms
B
ASIC-SC amplitude (pA)
0
10
20
30
40
50
60
Control
AZT

Figure 2

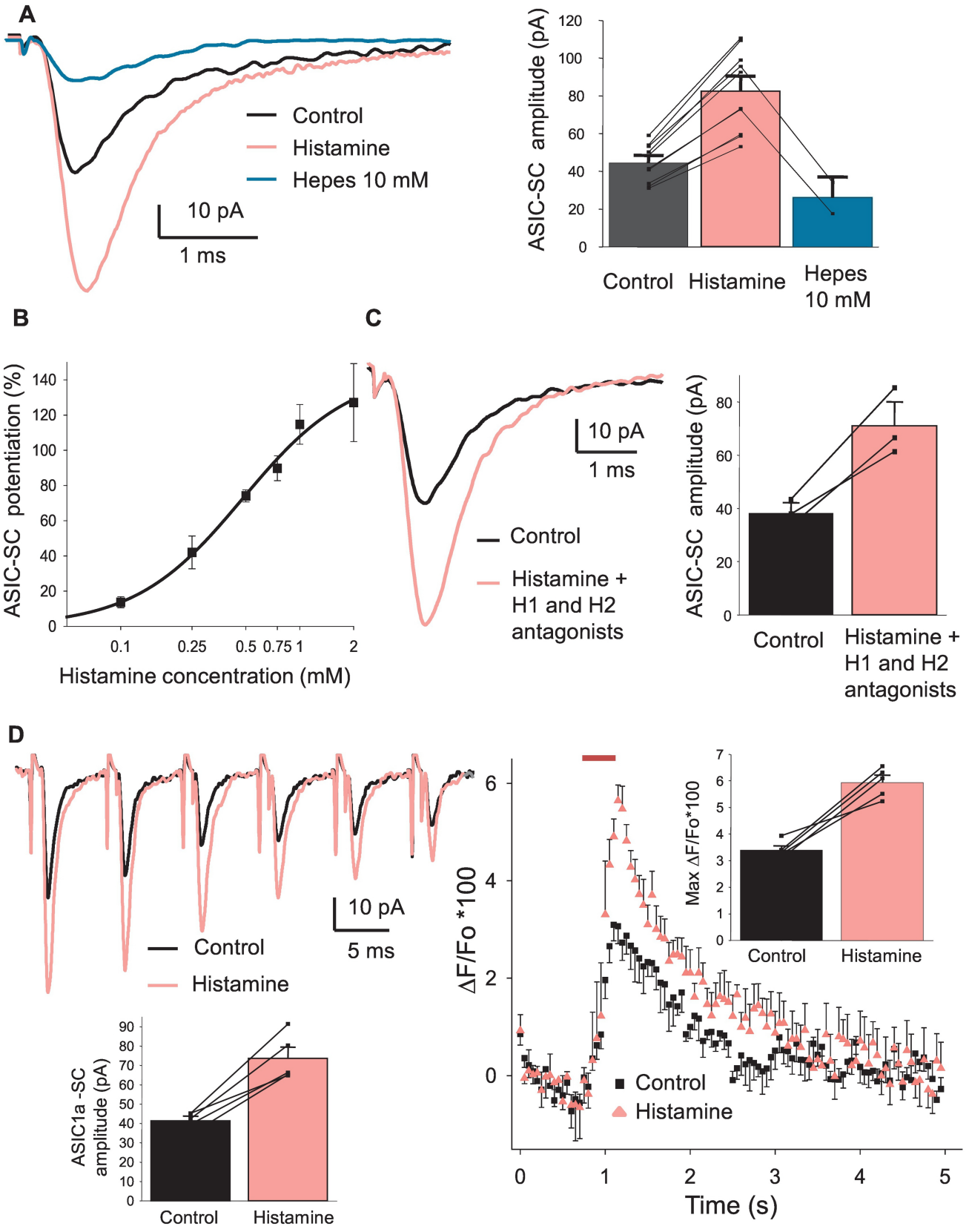
A
Control
Histamine
Hepes 10 mM
10 pA
1 ms
ASIC-SC amplitude (pA)
120
100
80
60
40
20
0
Control
Histamine
Hepes 10 mM
B
ASIC-SC potentiation (%)
140
120
100
80
60
40
20
0
0.1
0.25
0.5
0.75
1
2
Histamine concentration (mM)
C
10 pA
1 ms
Control
Histamine + H1 and H2 antagonists
ASIC-SC amplitude (pA)
80
60
40
20
0
Control
Histamine + H1 and H2 antagonists
D
10 pA
5 ms
Control
Histamine
ASIC1a -SC amplitude (pA)
90
80
70
60
50
40
30
20
10
0
Control
Histamine
ΔF/Fo *100
6
4
2
0
Control
Histamine
0
1
2
3
4
5
Time (s)
Max ΔF/Fo*100
7
6
5
4
3
2
1
0
Control
Histamine

Figure 3

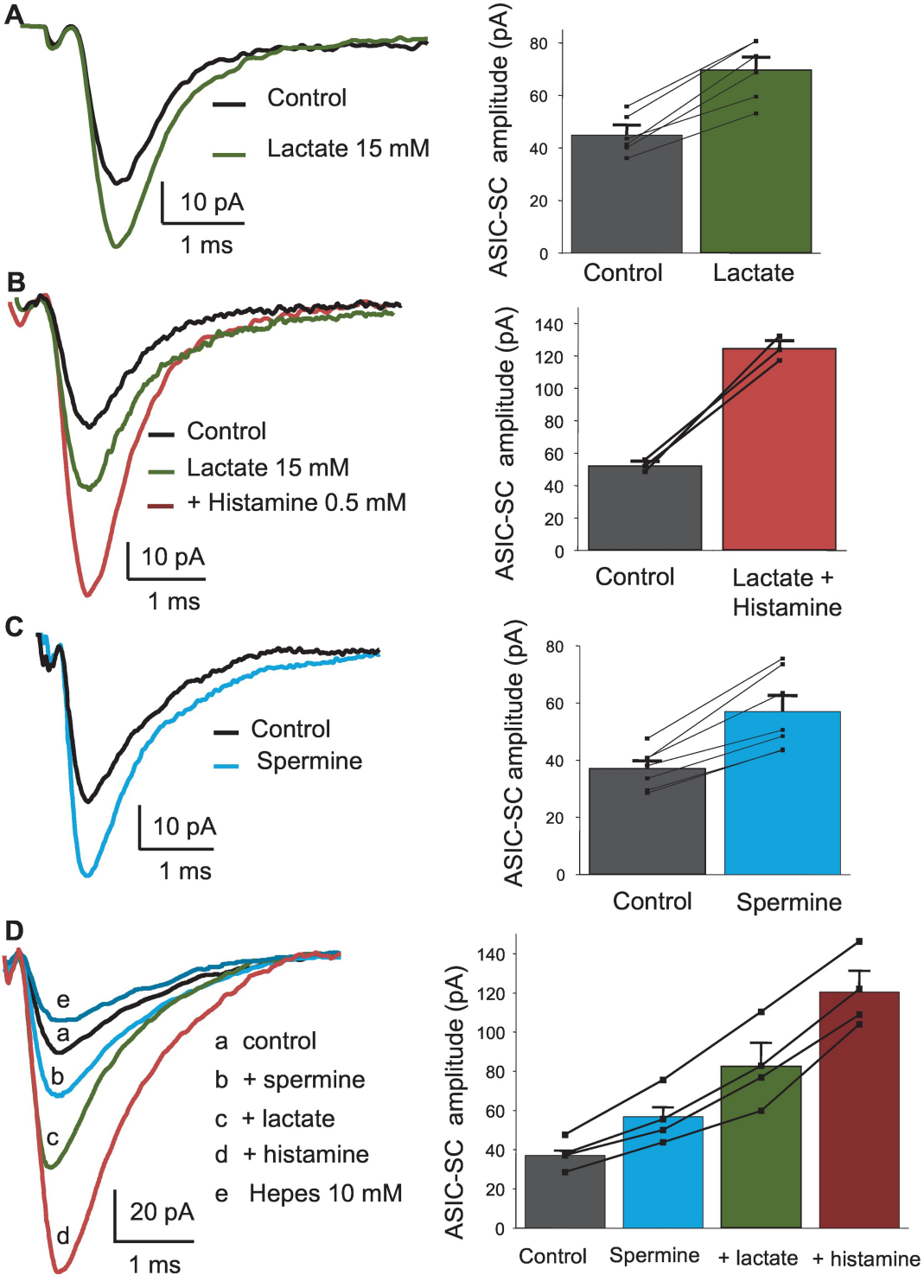
A
Control
Lactate 15 mM
10 pA
1 ms
ASIC-SC amplitude (pA)
Control
Lactate
B
Control
Lactate 15 mM
+ Histamine 0.5 mM
10 pA
1 ms
ASIC-SC amplitude (pA)
Control
Lactate +
Histamine
C
Control
Spermine
10 pA
1 ms
ASIC-SC amplitude (pA)
Control
Spermine
D
e
a
b
c
d
a control
b + spermine
c + lactate
d + histamine
e Hepes 10 mM
20 pA
1 ms
ASIC-SC amplitude (pA)
Control
Spermine
+ lactate
+ histamine

Figure 4

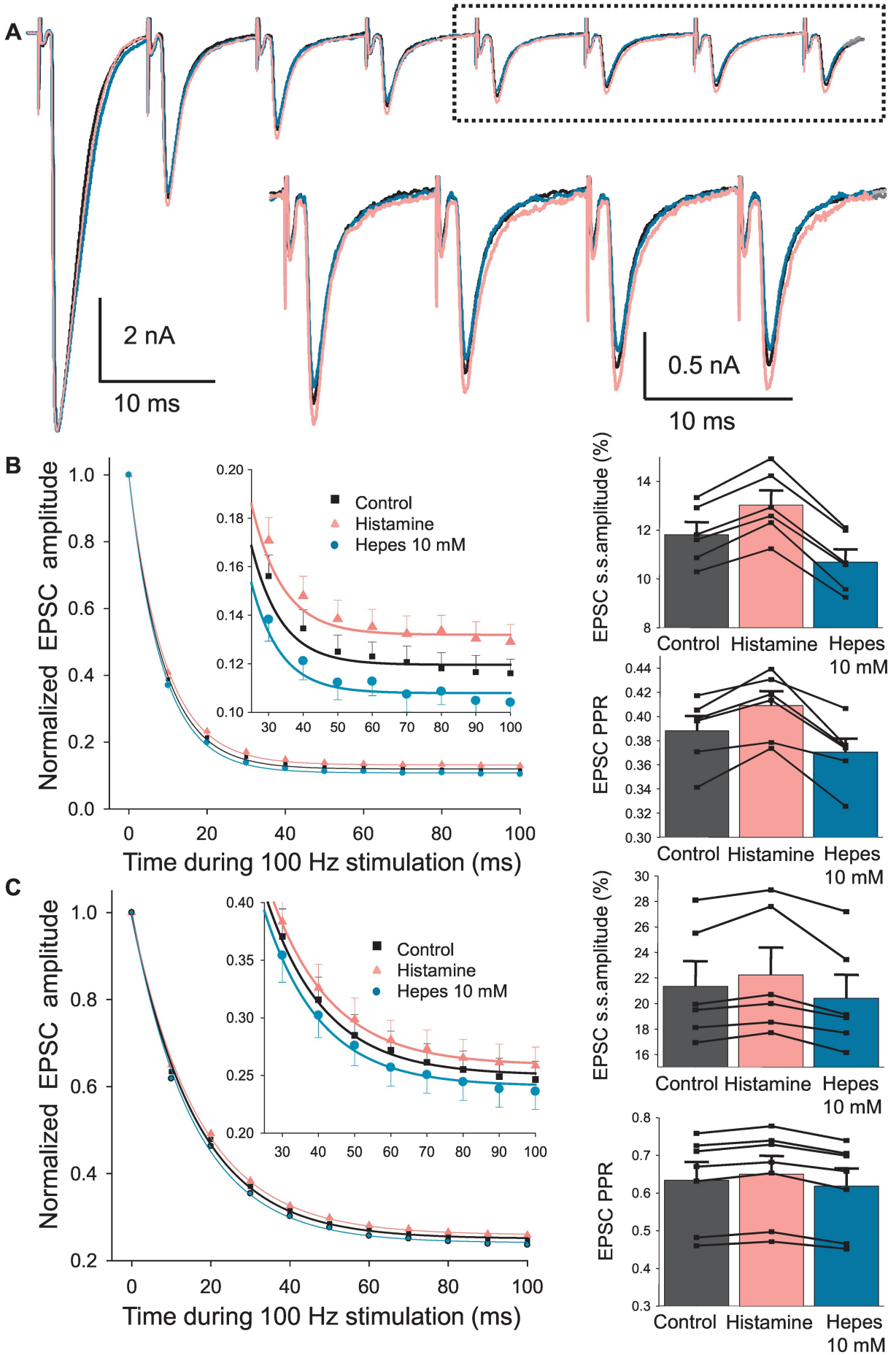
A
2 nA
10 ms
0.5 nA
10 ms
B
Normalized EPSC amplitude
Control
Histamine
Hepes 10 mM
Time during 100 Hz stimulation (ms)
EPSC s.s.amplitude (%)
Control Histamine Hepes 10 mM
EPSC PPR
Control Histamine Hepes 10 mM
C
Normalized EPSC amplitude
Control
Histamine
Hepes 10 mM
Time during 100 Hz stimulation (ms)
EPSC s.s.amplitude (%)
Control Histamine Hepes 10 mM
EPSC PPR
Control Histamine Hepes 10 mM

Figure 5

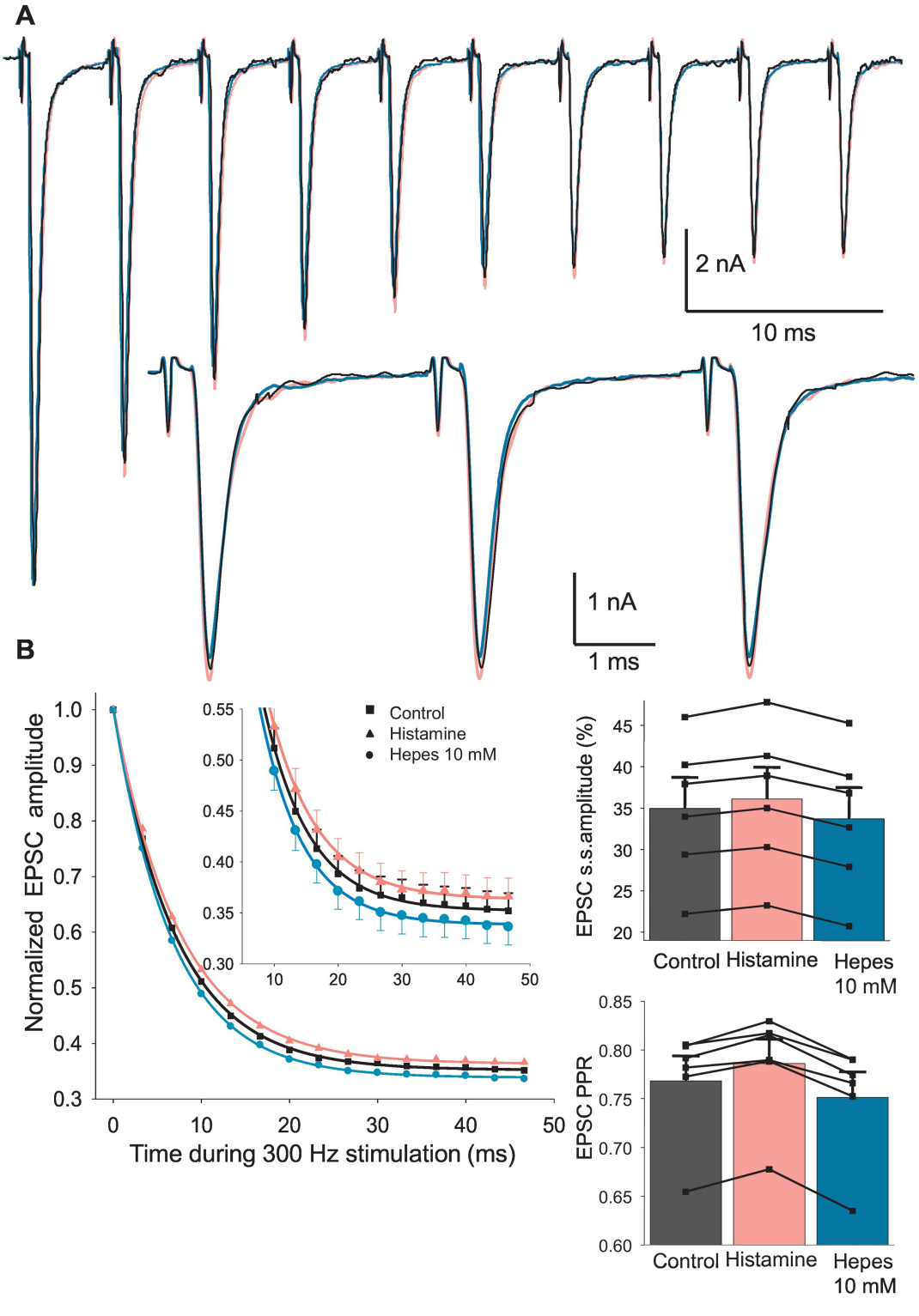
A
2 nA
10 ms
1 nA
1 ms
B
Normalized EPSC amplitude
Time during 300 Hz stimulation (ms)
Control
Histamine
Hepes 10 mM
EPSC s.s.amplitude (%)
Control Histamine Hepes 10 mM
EPSC PPR
Control Histamine Hepes 10 mM

Figure 6

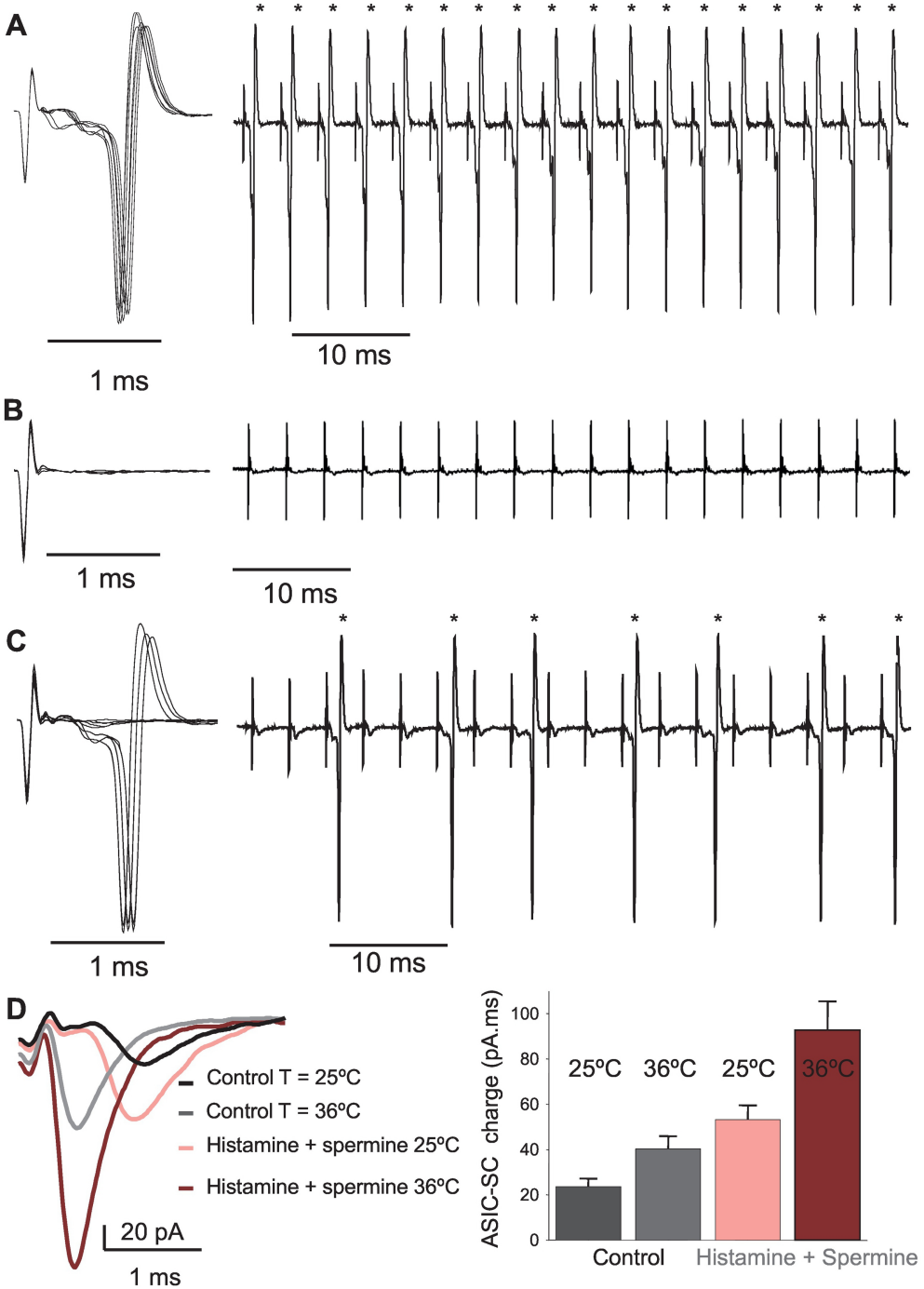
A
1 ms
10 ms
B
1 ms
10 ms
C
1 ms
10 ms
D
Control T = 25ºC
Control T = 36ºC
Histamine + spermine 25ºC
Histamine + spermine 36ºC
20 pA
1 ms
ASIC-SC charge (pA.ms)
100
80
60
40
20
0
25ºC
36ºC
25ºC
36ºC
Control
Histamine + Spermine

Figure 7